Ground-Based Light Curve Follow-Up Validation Observations on TESS Object of Interest TOI-3798.01

Alex Choi[1], Nate Vailikit[1], and Dr. Peter Plavchan[2]

[1]Woodson High School, 9525 Main Street, Fairfax, VA 22031, USA

[2]Department of Physics and Astronomy, 4400 University Drive MS 3F3, George Mason University, Fairfax, VA 22030, USA

August 3, 2024

Abstract

Exoplanet candidates are planets discovered outside the defined solar system that have only been proven to exist once confirmed by additional telescope observation. The Transiting Exoplanet Survey Satellite (TESS) under the National Aeronautics and Space Administration (NASA) Explorers Program surveys the surrounding sky for such exoplanet candidates via transit detection and machine learning techniques. TESS Object of Interest (TOI) 3798.01 (the particular focus of this study) was marked as a candidate exoplanet by TESS around a host star (TOI-3798) in 2021. The objective of this study was to perform a follow-up validation observation of TOI-3798.01. Such follow-up validation was utilized to sufficiently determine whether the TOI was deemed a false positive or a confirmed exoplanet. George Mason University's (GMU's) 0.8-meter telescope was operated to collect data on TOI-3798.01, mostly in the Flexible Image Transport System (FITS) data format which is used in the field of astronomy to store, transmit, and process data sets. Software such as AstroImageJ (a data science software tailored to astronomical imaging) and Ansvr (a plate-solving software for Windows operating systems) were then utilized to analyze such data and generate visualizations (particularly seeing profiles and light curve plots) to determine the existence of an exoplanet via the transit detection method. Approximately 30 minutes into the observation, the suspected transit occurred, long before the event was predicted to occur. Unfortunately, due to the absence of many of the stars provided by *Gaia* in the image and the apparent dimness of the others, the NEB check was inconclusive. However, in analyzing the data provided by TESS, the plot passes the visual odd/even test which is a quick and easy way to rule out eclipsing binary star systems. If validated through future studies, TOI-3798.01 would most likely be a hot Jovian with condensing Zinc Sulfide (ZnS).

1. Introduction

Within the field of astronomy, exoplanets (planets outside of the solar system) have been significant in supplementing the human understanding of planetary systems (including the solar system). The first indisputably confirmed exoplanet was in 1995 via the radial velocity method (Doppler Spectroscopy) [1]. The Milky Way galaxy is estimated to include hundreds of billions of exoplanets, despite only over five thousand and three hundred being discovered through common techniques such as radial velocity and transit methods [1]. TESS, a part of the NASA Explorers Program, launched in 2018 to identify thousands of exoplanets around bright host stars and near the solar system [2]. TESS utilizes the transit method, monitoring hundreds of thousands of stars for measurable dips in light output based on exoplanets crossing in front of stars from the perspective of TESS [2]. However, unlike the Hubble Space Telescope, which also used the transit method, TESS instruments gather a sufficient amount of photons to conduct spectroscopy which has allowed astronomers to discover the composition, history, climate, and habitability of such exoplanets [2]. Ephemerides of exoplanets also provide precise predictions of the exoplanets' positions and movements, essential for planning observations and studying the orbits and characteristics of such exoplanets. When TESS discovers an exoplanet, it is designated as a TOI (Tess Object of Interest) that must undergo a candidate validation process as TESS light curves (which measure the dips in a star's light output) can often result from a false positive. Such false positives include brown dwarfs, blended stellar binaries, and grazing stellar binaries. Exoplanet candidates are thereby comprehensively observed from additional telescope observations, with further analysis able to detect or rule out false positive scenarios.

The additional telescope observations, mostly ground-based telescope observations, also allow for further spectroscopy and thus the determination of the classifications of such TOIs.

One example is the study of TOI-4620.01, a “hot Jupiter” with temperatures around 2912.350 kelvin (K), an orbital period of 1.389 days, and a radius of 3.642 earth radii ($R_{\oplus}$) [3]. This study utilized observations from the GMU 0.8-meter telescope, generating and analyzing a ground-based light curve to validate and classify the “hot Jupiter” TOI [3]. Another example is the study of TOI-3353.01 and TOI-3353.02, both were originally suspected as false positives due to eclipsing binaries, though analyzed based on stellar density to be a confirmed multi-planetary system [4]. Thousands of TOI candidates have not been analyzed, meaning that such candidates are not entirely qualitatively understood based solely on TESS data compared to both examples with extensive ground-based follow-up validation observations.

In the study of the TOI-3353 planetary system, both TOIs were validated probabilistically through the *Gaia* (Global Astrometric Interferometer for Astrophysics) Early Data Release 3 and on-off photometry observations, even though the system was suspected to contain false positives [4]. Such false positives have resulted from the low spatial resolution of TESS’s cameras, which is approximately 21 arcseconds per pixel [4]. Additionally, stars crowded within TESS’s 1 arcminute^2 point spread function can merge stars into its time series, thus potentially diluting the transit signal, making the TOI seem like an eclipsing binary or an exoplanet [4]. The focus of this paper, TOI-3798.01, has not previously been included in a publication. Thus, we observe and analyze TOI-3798.01 in this paper based on TESS and the GMU 0.8-meter telescope to potentially validate and classify this exoplanet because of the need for TESS candidate ground-based follow-up validation observations.

In this paper, we present follow-up observations of TOI-3798.01. TOI-3798.01 has a planet radius (R_p) of 12.2250 $R_{\oplus}$ or 1.0906 Jupiter radii (R_{Jup}) and an orbital period (P) of 2.6797 days [5]. TOI-3798, the host star, is a G-type main-sequence star as its stellar effective

temperature (T_{eff}) is 5573.000 K and has a stellar radius ($R_\star$) of 1.0755200 solar radii ($R_\odot$) [5]. Ultimately, our goal is to investigate whether or not the transit occurs on the expected star (TOI-3798) at the expected time, with the expected duration and depth.

Section 2 presents our observations from TESS and the GMU 0.8-meter telescope. In section 3, we present our analysis of the TESS light curve for TOI-3798.01 along with our ground-based light curve analysis. In section 4, we present our light curve results. In Section 5 we discuss our results from the light curve. Lastly, in section 6, we present our conclusions and future work.

2. Observations

Section 2.1 presents the stellar properties of TOI-3798 and its candidate exoplanet's properties from the TESS Input Catalog (TIC). In section 2.2, we present the TESS sector light curve. Finally, in section 2.3, we present a summary of the TOI's observational data collected with the GMU 0.8-meter telescope.

2.1. Host Star Properties and Candidate Exoplanet Properties

In 2021, TESS identified a potential exoplanet orbiting its stellar host TOI-3798, also known as TIC 22683951, during a routine observation [5]. This star is located at right ascension (RA) 08 hour (h)16 minute (m)27.58 second (s) and declination (DEC) +47d01m19.16s [5]. TOI-3798 has a T_{eff} of 5573.000 K, an $R_\star$ of 1.0755200 $R_\odot$, and a stellar mass ($M_\star$) of 0.98000000 solar masses ($M_\odot$) [5]. The candidate exoplanet, TOI-3798.01, has a P of 2.6797 days, a R_p of 12.2250 $R_\oplus$ or 1.0906 R_{Jup}, a transit duration (T_{14}) of 2.0292 d, an equilibrium temperature (T_{eq}) of 1316.5339 K, and a depth of 9857.9234 parts per million (ppm) [5].

2.2. TESS Sector Light Curve

Using the Mikulski Archive for Space Telescopes (MAST) portal, a public database provided by the Space Telescope Science Institute (STScI), data on TOI-3798.01 observed by TESS was retrieved. This particular observation began on 2021 December 31 at a time of 7:39:58. Additionally, with the use of AstroImageJ, a light curve plot was created of TOI-3798.01 based on the data retrieved.

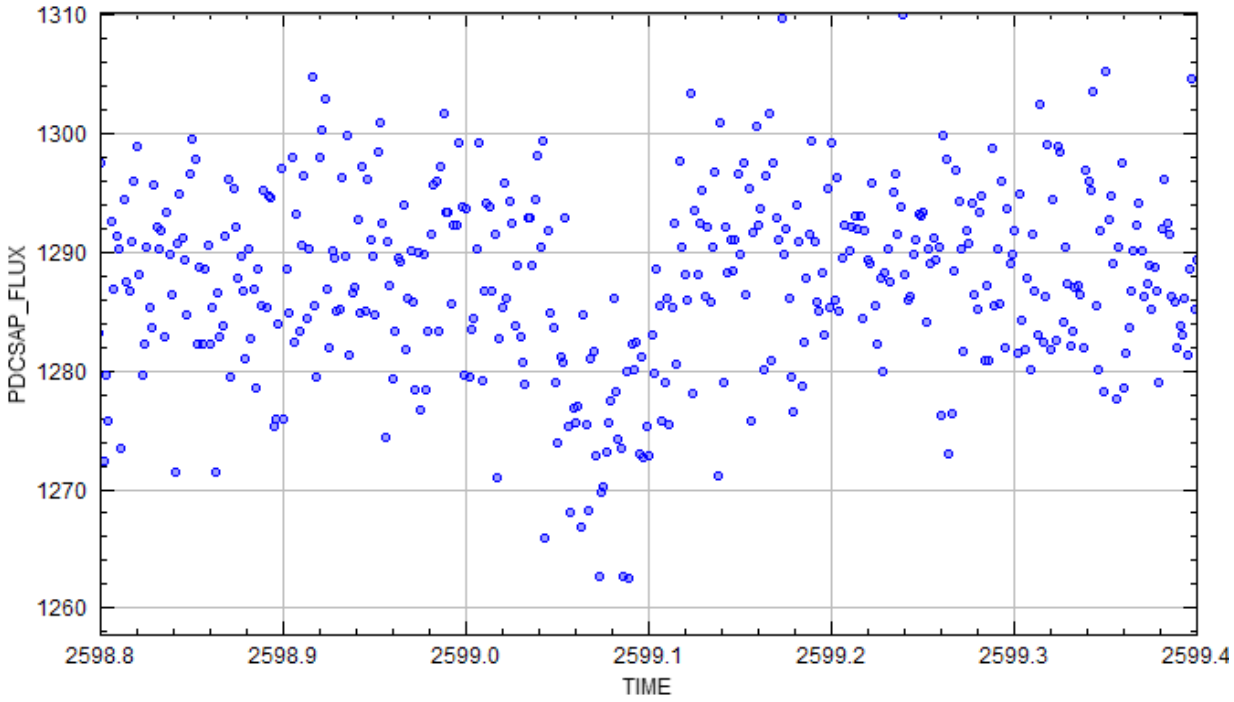

Figure 1. TESS light curve for TOI-3798.01 in sector 47.

2.3. Observational Data from GMU's 0.8-meter Telescope

GMU's 0.8-meter telescope was also utilized for observational data collection, being geographically located at -77°18′19.24″ West (W) longitude, +38°49′41.5″ North (N) latitude, with an altitude of 148.72 meters. TOI-3798.01 was observed by GMU's 0.8-meter Telescope through a red (R) filter, on 2024 February 5. The observation began at 18:35 EST and concluded at 6:10 EST the next morning. The predicted ingress time was 23:29, and the predicted egress

time was 1:03 the next morning. Thus, the predicted transit duration was 1 hour and 34 minutes. In total, 165 sciences were taken at an exposure time of 85.0 s each. The frame of exposure number 18 was removed during data reduction due to a telescope's movement during the capture of exposure number 18.

3. Analysis

Section 3.1 presents the tools used to analyze the data collected by GMU and TESS for TOI-3798.01 using AstroImageJ and the odd/even test. In section 3.2 we present our analysis of the quality of the collected data over time. In Section 3.3, we ultimately present our ground-based light curve analysis using AstroImageJ's plotting tools.

3.1. Tools for Data Analysis

AstroImageJ, the software used for our data analysis, is a graphical user interface Java-based software package utilized for image calibration and data reduction specifically in astronomy, while also emphasizing several streamlined tools for exoplanet transits [6]. Such tools used in our analysis include multi-aperture photometry and light curve plotting, detrending, and fitting, thus allowing for the creation of precise light curves for TOI-3798.01 [6].

Initially, the AstroImageJ data processor allowed us to median combine darks and flats to reject cosmic rays and reduce noise by a factor of about 3. Then, we created a dark subtracted flatfield (median-combined flatfield subtracted by the median combined darks with the same exposure time) to remove the electronic detector signal, thus isolating the electrons generated by the photons. Next, we normalized the flatfield (where the dark subtracted flatfield is divided by the median value of the illuminated part of the dark subtracted flatfield), which turned the flatfield image into a pixel correction image of what percentage of light is reported by each pixel, thus removing variation in counts for the flat fields. Afterward, we dark subtracted the science

images to isolate the electrons again. Finally, we created reduced science images (where the dark subtracted science images are divided by the reduced flat fields) to remove the variation in individual pixels, thus allowing the differently behaving pixels to report the same number of counts as the photons.

With the reduced science images, using the astrometry feature, AstroImageJ has allowed us to plate solve the FITS science images by sending coordinates of bright sources to astrometry.net, ultimately returning a list of sources and adding World Coordinate System (WCS) headers to the science images that we then analyzed using the tools as mentioned earlier [6].

Additionally, an odd/even test was conducted for TOI-3798.01 as one way to check for the possibility of an eclipsing binary. In the odd/even test, the folded light curve for TOI-3798.01 was separated into the odd-numbered transits (e.g., transit one, transit three, transit five) and the even-numbered transits (e.g., transit two, transit four, transit six) [7]. TOI-3798.01 would most likely exhibit an exoplanet if the odd and even transits exhibited identical shapes and depths as the orbit of TOI-3798.01 would be periodic and consistent [7]. However, the odd and even transits differing would indicate an eclipsing binary star as the behavior of such stars would not be periodic and consistent in the odd/even plots [7].

3.2. Quality Analysis of Collected Data Over Time

During the observation on February 5th, 2024, the quality of the exposures noticeably decreased during the duration of the image capturing. A blurring of the images gradually occurred during the night with no clear start (as shown in Figure 6), making the reduction and interpretation of data past this point very difficult. See Figure 2a (Frame 1) and Figure 2b (Frame 164) below.

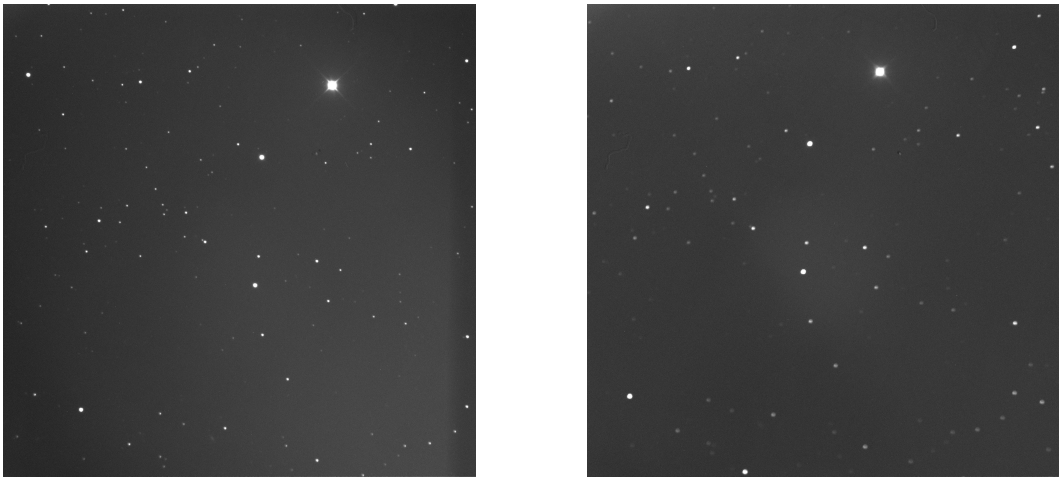

(a) **(b)**

Figure 2. Exposure frames for TOI-3798.01. **(a)** Frame 1. **(b)** Frame 164.

The difference between frame 1, as seen in Figure 2a, and frame 164, as seen in Figure 2b, is qualitatively different as apparent in the reduced sharpness of the exposure frame. On the other hand, the quantitative difference between the star TOI-3798 in frame one versus frame 164 can be represented by comparing the plots generated by AstroImageJ of both frames. Seeing profile plots in AstroImageJ allowed us to measure the aperture and annulus radius of TOI-3798.01. Figure 3a below, the plot of TOI-3798.01 in frame 1, is deeper and the sample radius extends into the background. However, in Figure 3b below, the seeing plot of TOI-3798.01 in frame 164, is shallower and the sample radius barely extends into the background, corresponding with the reduced sharpness evident in Figure 2b.

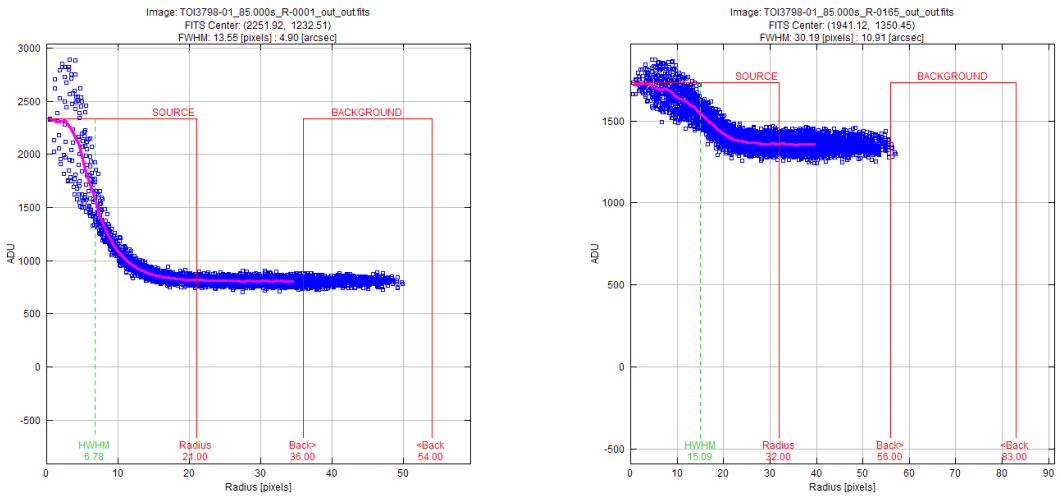

(a) **(b)**

Figure 3. Seeing plots for TOI-3798.01. **(a)** Frame 1. **(b)** Frame 164.

The cause of this reduced sharpness was not reported. See Figure 4 below for the graph of the full-width half maximum (FWHM) over time created in AstroImageJ. FWHM, the width of a Gaussian (normal) distribution bell curve at half its maximum value (the bell curve being the star's brightness over a centered cross-section of the image sample), is a more definitive representation of star sharpness. Equation (1) below shows the relation between the FWHM and the standard deviation of the normal distribution function.

$$FWHM = 2\sigma\sqrt{2ln(2)} \approx 2.3548\sigma \quad \textbf{(1)}$$

where σ = standard deviation

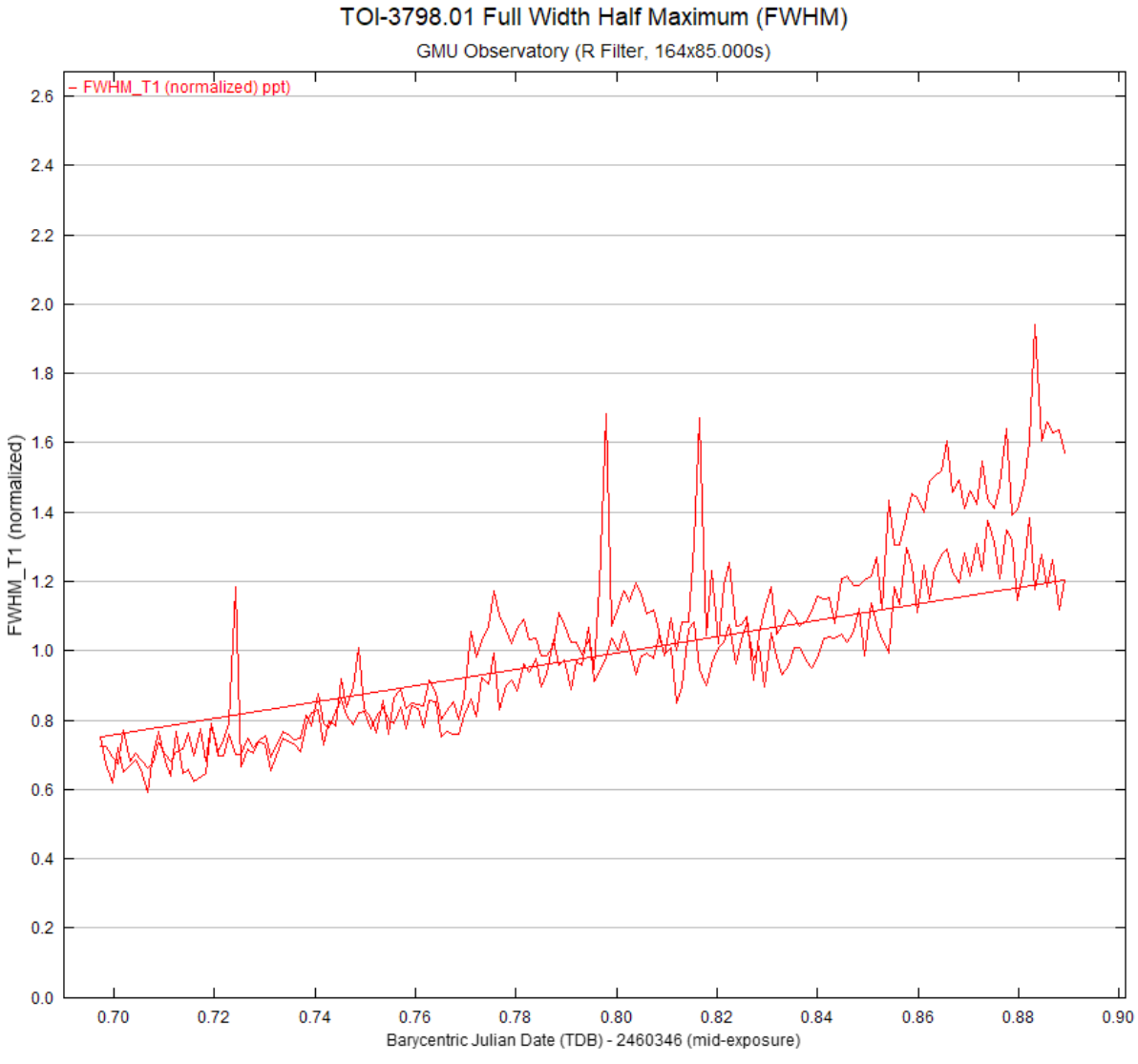

Figure 4. FWHM for TOI-3798.01 over time.

3.3. Ground-Based Light Curve Analysis Using AstroImageJ

Multi-aperture photometry in AstroImageJ has allowed for the plotting, detrending, and fitting of the light curve for TOI-3798.01.

Beforehand, we used the aperture photometry tool to select our target star (TOI-3798), which then opened a window showing the profile plot of TOI-3798.01, showing the radius, inner annulus, and outer annulus values of the target (see Figure 3 for two seeing profile plots). We then changed the aperture photometry settings, where the three given values were inputted, along with the specifications of GMU's 0.8-meter telescope camera's charge-coupled device (CCD).

Next, we placed a 2.5-inch radius circle around TOI-3798 and placed a *Gaia* .radec file with *Gaia* stars. We then opened the multi-aperture photometry tool to enter multi-aperture measurements and place apertures, allowing us to conduct differential photometry. Afterward, reference stars of similar brightness and size away from the edge of the images were selected. Finally, data was measured into a measurements table that allowed for the creation of the light curve plot. Ultimately, differential photometry allowed us to avoid calibrating our data concerning another magnitude standard. Equation (2) below shows how AstroImageJ calculates the average correction factor based on the difference between the true and instrumental magnitudes of the standard stars, finally applying this correction to the instrumental magnitude of the target star to estimate its true magnitude.

$$M_{true}(target) = M_{inst}(target) + \frac{1}{N}\sum_{i=1}^{N}(M_{true}(standard_i) - M_{inst}(standard_i)) \qquad \textbf{(2)}$$

where M_{true}(target) = the true magnitude of the target star, M_{inst}(target) = the instrumental magnitude of the target star, M_{true}(standard$_i$) = the true magnitude of the *i*-th standard star,

$M_{inst}(standard_i)$ = the instrumental magnitude of the i-th standard star, and N = the number of standard stars used.

Then, the multiplot tool was used to go to a multi-plot main window to input the predicted ingress and egress times. The data set 2 fits settings window was then used to input parameters concerning the host star and the planet, TOI-3798.01. The multi-plot-y-data window was then utilized to enter the recommended scale, shift, and colors for several y-data parameters (see Figure 8 for all parameters used) along with the review of the flux of reference stars to note stars with large variation or scattering. The multi-plot reference star settings window was used to remove such noted stars. The TESS Follow-Up Observing Program (TFOP) Sub-Group 1 (SG1) Nearby Eclipsing Binary (NEB) Analysis Macro window was then used to create a delta magnitude (Dmag) root mean square (RMS) plot to identify any outlier stars. An NEB check and Dmag vs RMS plots (Figure 5 below) were then followed to rule out a potential false positive of an NEB.

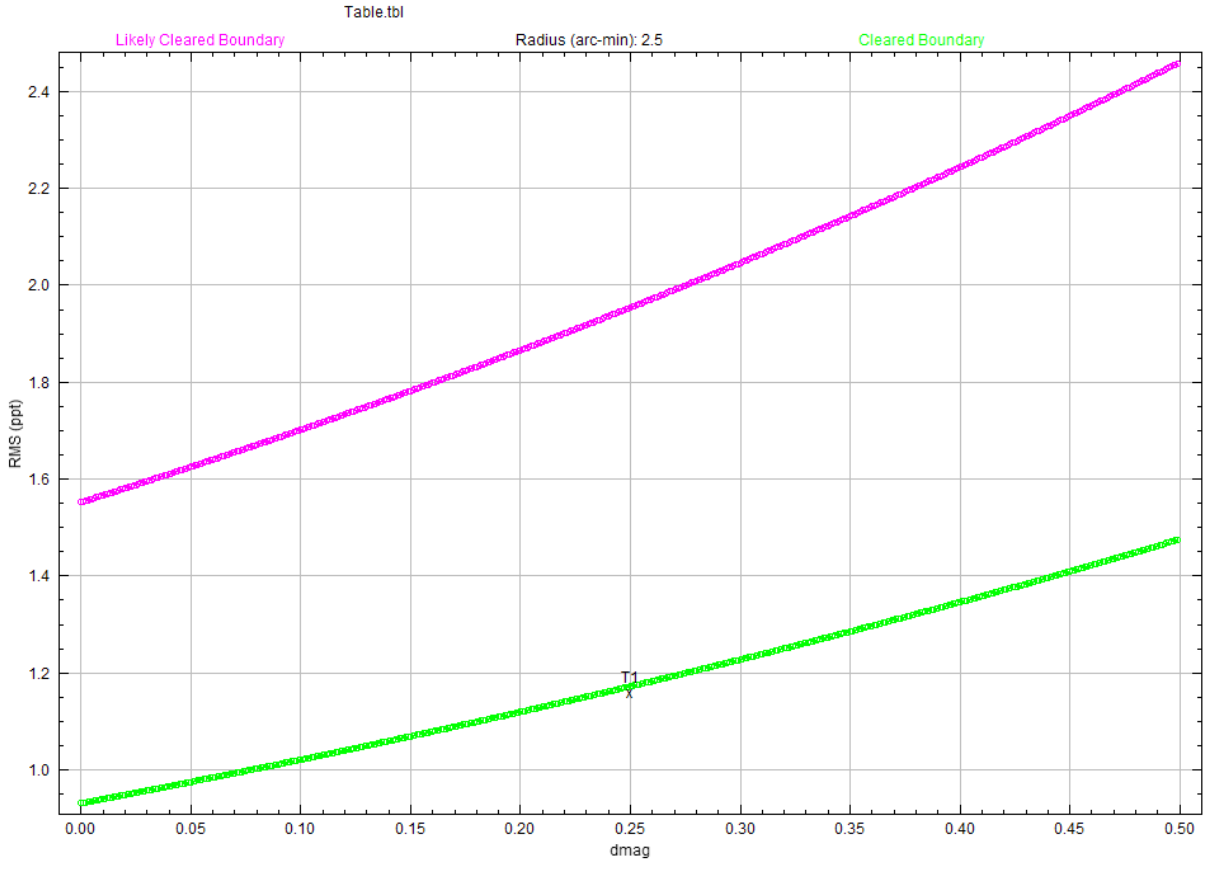

Figure 5. Dmag vs RMS plot of the target T1 (TOI-3798.01).

Figure 5 does not include the *Gaia* stars due to the lack of such stars within the field of view (FOV) and the apparent dimness of the stars used in the NEB check, as evident in Figure 6 below.

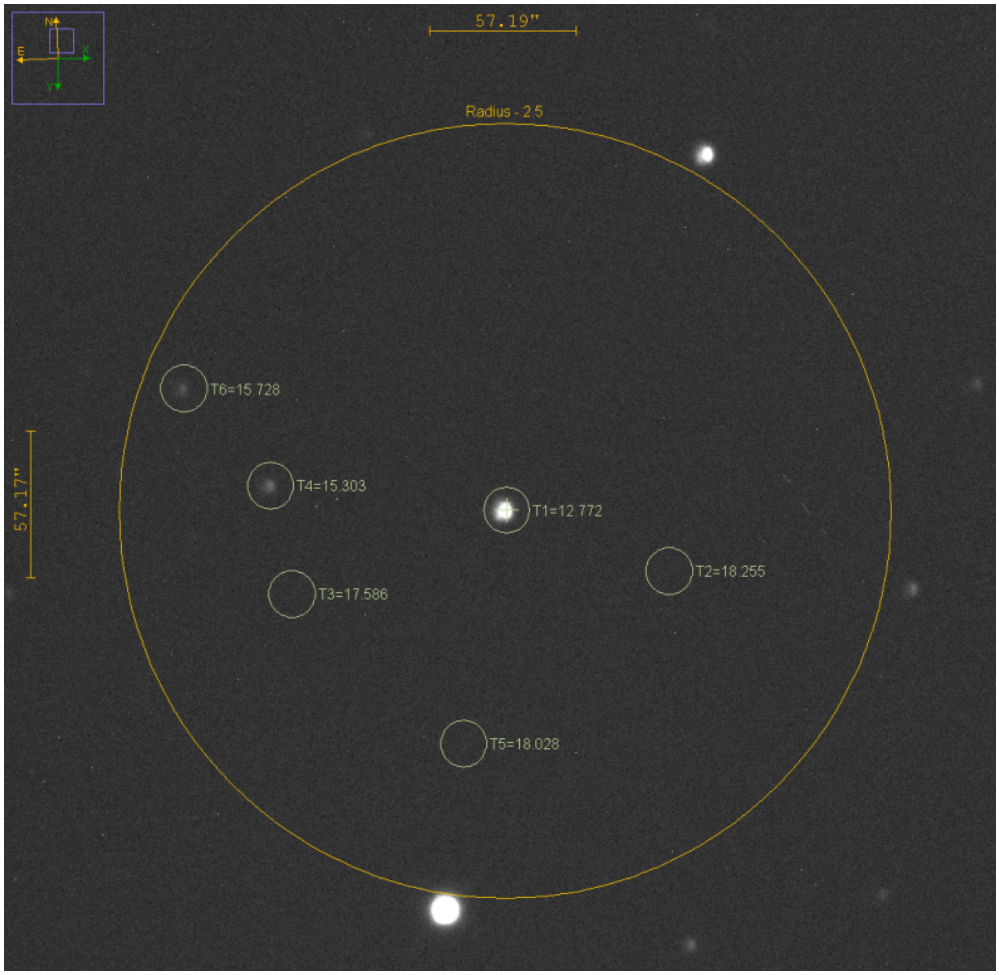

Figure 6. The *Gaia* reference stars, highlighted in green circles, excluding T1 (TOI-3798.01), were too dim and some are missing.

Figure 7 below, the NEB depth plot for TOI-3798.01, shows the depth of potential eclipses caused by eclipsing binary stars relative to the target star, T1, supplementing in the identification of a false-positive.

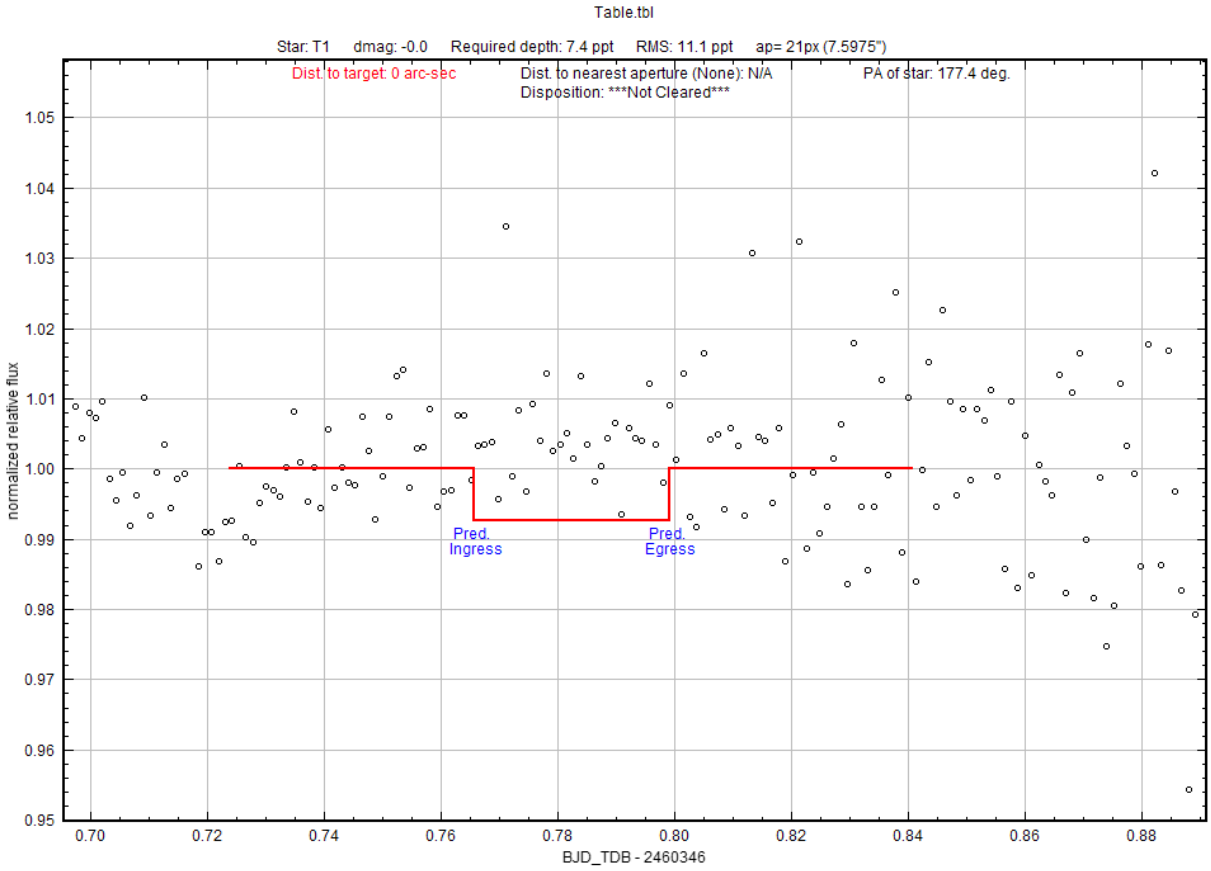

Figure 7. NEB depth plot for T1 (TOI-3798).

4. Results

Performing multi-aperture photometry to create a light curve of TOI-3798.01 allowed for the creation of several plots that are a part of the light curve. See Figure 8 below for the light curve plots. The first plot is the normalized flux of T1, which is TOI-3798.01, compared to reference stars over exposure time. The second plot shows the air mass detrending with a transit fit, representing the atmospheric thickness of TOI-3798.01 which light travels through. The third plot is the transit model for TOI-3798.01, showing how much the light curve fits this transit. The fourth plot shows residuals (the differences between the predicted and actual flux) utilizing the chi^2 fit test. The fifth plot is of the x-coordinates of T1 over time. The sixth plot shows the air mass, representing the amount of atmosphere the GMU 0.8-meter telescope looks through before

the observation of TOI-3798.01. The seventh plot is of the width of T1 over time. The eighth and final plot represents the normalized flux for light in the sky over time.

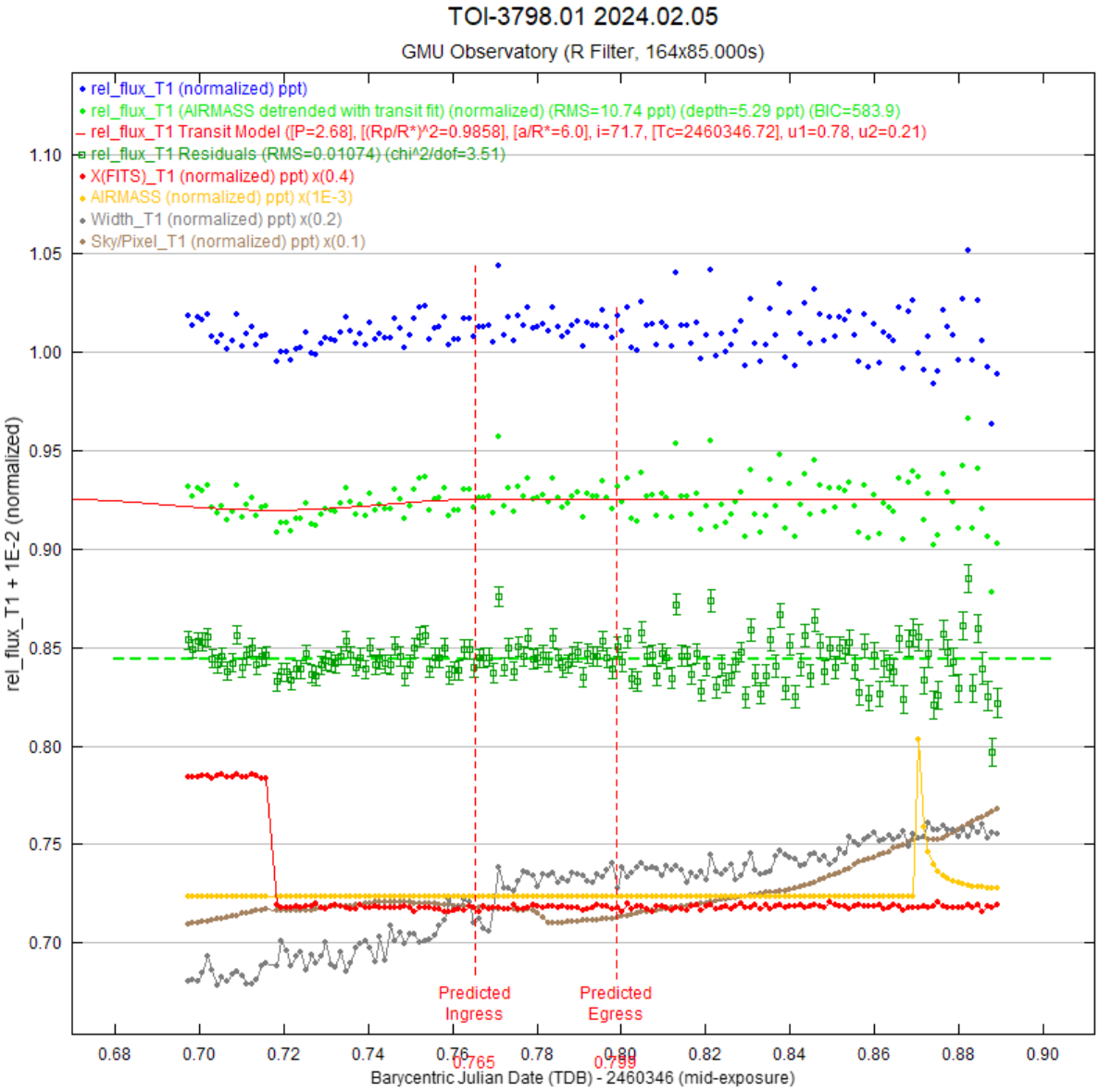

Figure 8. Light curve plot for TOI-3798.01.

The folded light curve for TOI-3798.01 based on the TESS median detrended time series (figure 9 below) represents the phase (days) versus flux (ppm).

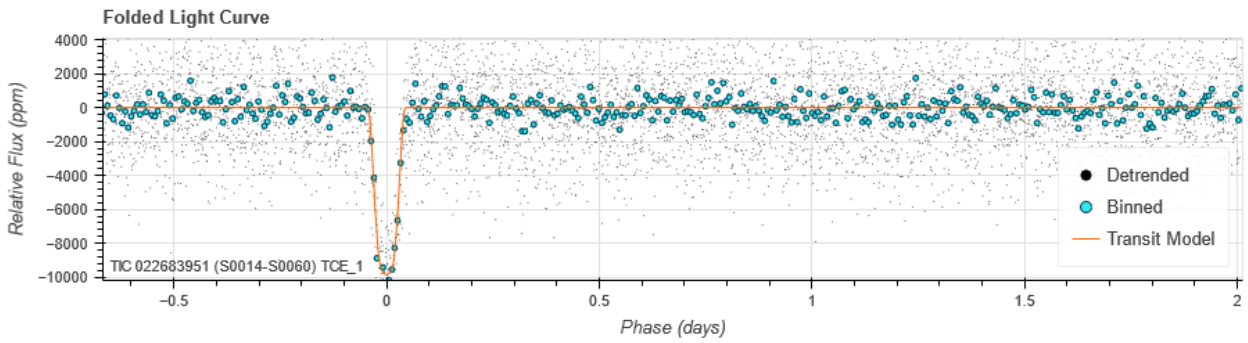

Figure 9. TESS Median Detrended Time Series Folded Light Curve for TOI-3798.01.

The odd and even plots (Figure 10) represent the odd and even-numbered transits of TOI-3798.01 from the folded light curve for TOI-3798.01 (Figure 9), which can be used to determine the possibility of an eclipsing binary signal.

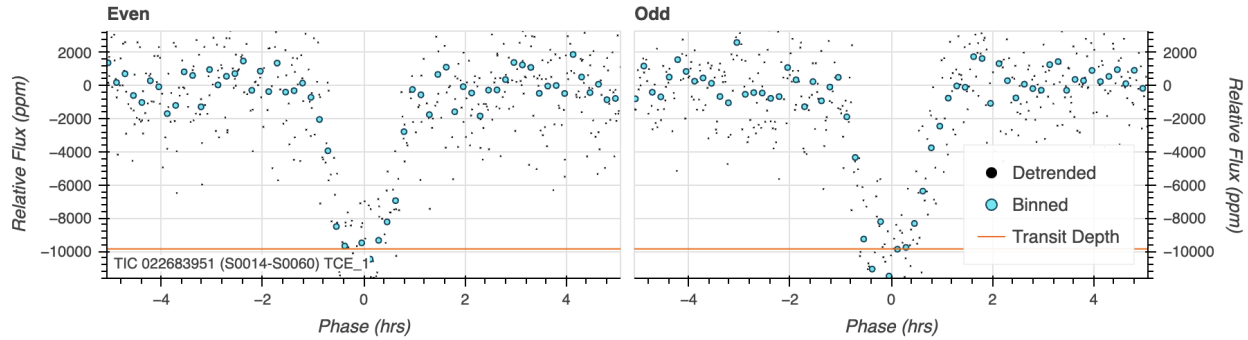

(a) **(b)**

Figure 10. TESS Median Detrended Time Series plots to conduct an odd/even test. **(a)** Even plot. **(b)** Odd plot.

5. Discussion

First, in section 5.1, we present our interpretation of the results. Then, in section 5.2, we contextualize our results in the greater field of the follow-up of candidate exoplanets from NASA TESS.

5.1. Interpretation of Results

In reviewing the reduced data, and the light curve plots, it was indeterminable whether or not an exoplanet transit occurred during the observation. Thus the possibility of a false positive as a result of an NEB remains unknown. There is a transit-like shape that occurs in the data between approximately x = 0.70 Barycentric Julian Date (TDB) and x = 0.74 TDB in Figure 8, although the NEB check failed due to the nearby star positions provided by the *Gaia* satellite containing stars that were far too dim to be used in the NEB check. Ultimately, three out of the five stars provided were not visible. The transit-like shape that did appear in the light plot was thereby unable to be confirmed as a false positive or not.

Though the NEB check was inconclusive, the odd/even test indicates that an eclipsing binary may not be likely as the shape of the odd plot mostly correlates with that of the even plot, thus showing a mostly even pattern between the two plots. However, the odd plot is very slightly more bowed downwards than the even plot due to the two lowermost binned points on the odd plot, though it does not deemphasize the correlating shape of the two plots. The time, duration, and depth of the TESS median detrended time series plots (Figure 9 and Figure 10) also match the expected time, duration, and depth, indicating the potential for exoplanet validation.

In addition, the predicted ingress and egress were not aligned with the true ingress and egress times apparent visually in Figure 8. Transit predictions showed the ingress time of x = 0.765 TDB and the egress time of x = 0.799 TDB. However, visually, the true ingress time appears to be around x = 0.70 TDB and the true egress time appears to be around x = 0.74 TDB. Equation (3) below is used to measure the accuracy of the ingress and egress times and the extent of the discrepancy between the predicted and true times.

$$\delta = \left|\frac{v_a - v_e}{v_e}\right| \cdot 100\% \quad \textbf{(3)}$$

where δ = the percent error, v_a = the theoretical value, and v_e = the experimental value

Using equation (3), the percent error for the ingress time is approximately 9.286% and the percent error for the egress time is $7.\overline{972}\%$. The discrepancy can be caused by atmospheric refraction, especially at observatories with high altitudes [8].

5.2. Contextualizing Results in Exoplanet Follow-Up Studies from NASA's TESS Mission

Based on the tentative results showing the possibility of TOI-3798.01 being an exoplanet, TOI-3798.01 would be classified as a "hot Jovian (Jupiter)" if further analyses and results allow for the validation of TOI-3798.01. Jovians have an $R_{\oplus}$ between 6.0 and 14.3, which TOI-3798.01 would fall under, having an $R_{\oplus}$ of 12.2250 [9]. The semi-major axis of TOI-3798.01 was found by multiplying the semi-major axis by the star radius ratio found on the A.2. of the Data Validation report for TOI-3798.01 (7.4932) by the star radius (1.07552 $R_{\star}$) to get 8.059 $R_{\star}$. Converting the semi-major axis to astronomical units (AU) was found by dividing the semi-major axis in $R_{\star}$ by dividing by 215, where the semi-major axis is approximately 0.038 AU. However, 0.038 AU was below the minimum value that the NASA Exoplanet Modeling Calculator could accept, which is 0.05 AU [9]. Regardless, this would remain in the theoretical "hot" range as a lower semi-major axis correlates with a higher stellar flux along with a closer distance to the host star. In addition, a different exoplanet, TOI-4620.01 was found to be a "hot Jupiter (Jovian)" with a semi-major axis of 0.0292 AU, a temperature of ~2912.350 K, and an orbital period of ~1.389 days [3]. In comparison, despite TOI-3798.01 not having as high of a temperature (~1316.53387 K < ~2912.350 K), TOI-3798.01 has an orbital period of ~2.680 days, which further indicates a "hot Jovian" as an orbital period of less than 10 days are typically attributed to "hot Jupiters" [3]. Ultimately, it is highly likely that TOI-3798.01 would be a "hot Jovian" if validated, as evident in the semi-major axis and orbital period of the exoplanet candidate.

Based on the high likelihood for TOI-3798.01 to be a “hot Jovian” if validated in future studies, it is then highly likely for TOI-3798.01 to have high contents of sphalerite zinc sulfide (ZnS) condensing into zinc (Z) as the stellar flux of TOI-3798.01 (~696.18 which was found by converting semi-major axis and luminosity into stellar flux) is greater than the condensation flux boundary for ZnS of 219.998 [9]. Additionally, per spectral features being determined by equilibrium chemistry, TOI-3798.01 most likely has a high atmospheric composition of hydrogen (H_2) and helium (He) as a “large planet” [9].

6. Conclusion and Future Work

The results of our observations showed a small dip in the relative flux of TOI-3798 occurring at approximately 7:00 PM, or x= 0.70 TBD. This event was unable to be defined as a false positive or an exoplanet transit. The NEB check, a tool provided by AstroImageJ, was used to rule out false positives, although the reference stars provided by *Gaia* were not sufficient to be able to properly execute a successful NEB check. This was due to the low apparent brightness of the stars, which can be seen in Figure 6. In reviewing data provided by ExoFOP TESS, there is no striking difference between the odd and even transits, although the difference that does occur is consistently alternating. Although, this difference is incredibly minimal and negligible at best. Ultimately, a transit-like event was observed, however, a false positive has not been ruled out by any means.

In retrospect, longer exposure images may have aided in the NEB check to verify the existence of an exoplanet. However, we must keep in mind that exposures that are too long can saturate the target star, and produce fewer data points in a single observation. In future studies, It would be beneficial to explore longer subframes not only to capture the target star but to capture the stars around it to be able to utilize the NEB check tool in AstroImageJ. In other

observations, routinely checking focus will prevent images from becoming blurred as they did during the imaging of TOI-3798, rendering much of the data unusable. Also in AstroImageJ, the predicted ingress and egress times should closely match the true ingress and egress times in future studies. The radial velocity method and subsequent spectroscopy can further reveal any possible false positives in future analysis. In addition, further statistical false-positive validation analysis (such as with the use of Bayesian statistics) and the potential use of deep learning algorithms can supplement in validating TOI-3798.01. TOI-3798.01 ultimately has the potential for further analysis into the planet's characteristics and composition if validated, which would supplement the growing investigation of "hot Jovian"' planets.

References

[1] Butler, P.R., & Traub, W.A. (2023, April). Exoplanet. AccessScience. Retrieved July 19, 2024, from https://doi.org/10.1036/1097-8542.800700

[2] AccessScience Editors. (2018, April). The Transiting Exoplanet Survey Satellite (TESS) mission begins. AccessScience. Retrieved July 19, 2024, from https://doi.org/10.1036/1097-8542.BR0418181

[3] Cao, D., Pich, L., & Plavchan, P. (2023). Ground-Based Light Curve Follow-Up Validation Observations of TESS Object of Interest (TOI) 4620.01. *Journal of Astro-Scholars Research (JASR)*, *1*, 58-69. https://doi.org/10.13021/MARS/2061

[4] Mantovan, G., Montalto, M., Piotto, G., Wilson, T. G., Cameron, A. C., Majidi, F. Z., Borsato, L., Granata, V., & Nascimbeni, V. (2022). Validation of TESS exoplanet candidates orbiting solar analogues in the all-sky PLATO input catalogue. *Monthly Notices of the Royal Astronomical Society*, *516*(3), 4432-4447. https://doi.org/10.1093/mnras/stac2451

[5] TIC 22683951. (n.d.). *ExoFOP*. Retrieved July 21, 2024, from https://exofop.ipac.caltech.edu/tess/target.php?id=22683951

[6] Collins, K. A., Kielkopf, J. F., Stassun, K. G., & Hessman, F. V. (2017). ASTROIMAGEJ: IMAGE PROCESSING AND PHOTOMETRIC EXTRACTION FOR ultra-precise ASTRONOMICAL LIGHT CURVES. *The Astronomical Journal*, *153*(2), 77. https://doi.org/10.3847/1538-3881/153/2/77

[7] Olaiz, E., & Plavchan, P. (2023). Ground-Based follow-up observations of TESS object of interest TOI 3779.1. *Journal of Astro-Scholars Research*, *1*, 70-82. https://doi.org/10.13021/MARS/2060

[8] Singh, J., & Plavchan, P. (2023). Transit method analysis for exoplanet detection validation observations for TESS object of interest 3553.01. *Journal of Astro-Scholars Research*, *1*, 103-108. https://doi.org/10.13021/MARS/2058

[9] Kopparapu, R. K., Hébrard, E., Belikov, R., Batalha, N. M., Mulders, G. D., Stark, C., Teal, D., Domagal-Goldman, S., & Mandell, A. (2018). Exoplanet classification and yield estimates for direct imaging missions. *The Astrophysical Journal*, *856*(2), 122. https://doi.org/10.3847/1538-4357/aab205